UNIVERSIDAD NACIONAL AUTÓNOMA DE MÉXICO

FACULTAD DE INGENIERÍA

AN EXPERIMENTAL NOTE ON THE DEFORMATION AND BREAKUP OF VISCOELASTIC DROPLETS RISING IN NON-NEWTONIAN FLUIDS

ARTICULO ACADEMICO

Que para obtener el título de

Ingeniera Mecánica

P R E S E N T A

ORTÍZ MARTÍNEZ SUSANA LUCIA

ASESOR DE ARTÍCULO ACADÉMICO

Dr. BALTAZAR MENA INIESTA

Ciudad Universitaria, Cd. Mx., 2017

Springer

An experimental note on the deformation and breakup of viscoelastic droplets rising in non-Newtonian fluids

Susana L. Ortiz, Julia S. Lee, Bernardo Figueroa-Espinoza & Baltasar Mena

Rheologica Acta

ISSN 0035-4511
Volume 55
Combined 11-12

Rheol Acta (2016) 55:879-887
00110.1007/s00397-016-0970-3

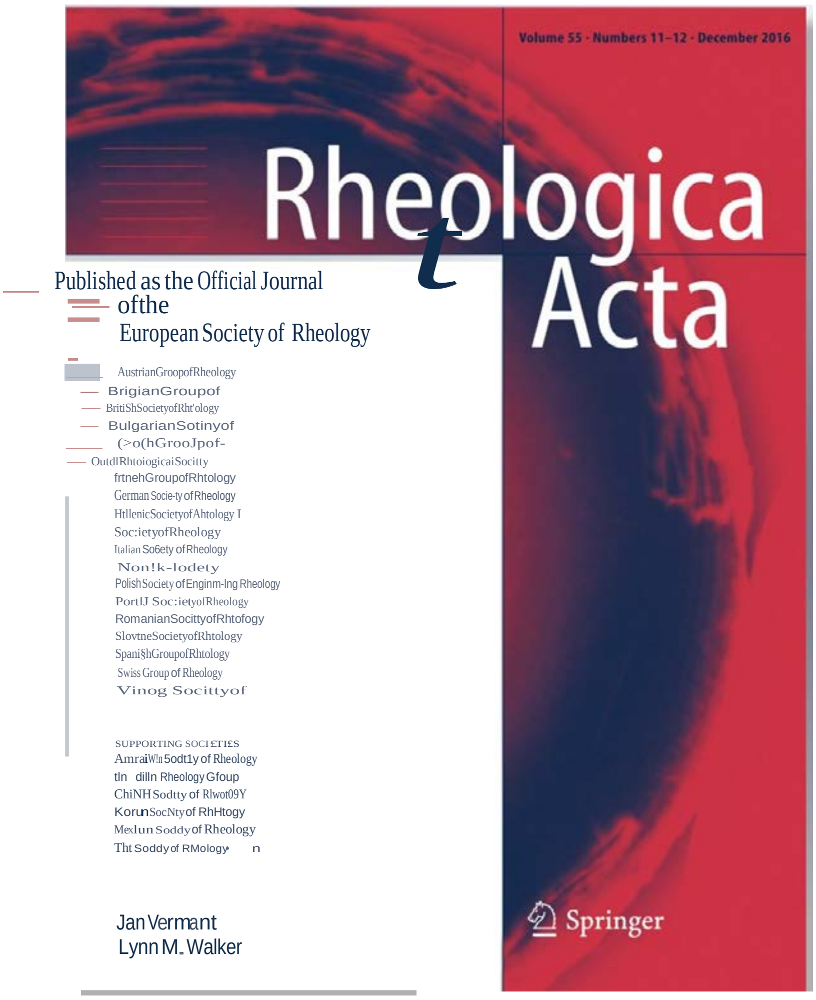

Springer

Rheol Acta (2016) 55:879–887
DOI 10.1007/s00397-016-0970-3

RAPID COMMUNICATION

An experimental note on the deformation and breakup of viscoelastic droplets rising in non-Newtonian fluids

Susana L. Ortiz [1] & Julia S. Lee [2] & Bernardo Figueroa-Espinoza [1] & Baltasar Mena [1]

Received: 2 May 2016 / Revised: 23 August 2016 / Accepted: 13 September 2016 / Published online: 7 October 2016

Abstract The deformation of viscoelastic droplets rising in non-Newtonian fluids is examined experimentally. Similarly to the case of bubbles and Newtonian droplets traveling in viscoelastic fluids, a critical volume exists but there is no jump in velocity nor a drastic change in droplet geometry. Nevertheless, a tail appears as well as a negative wake. For large-enough volumes, the thickness of the tail is much larger than that for the Newtonian droplets; this is also true for the magnitude of the negative wake and for the extension of the tail. The head of the droplet is subjected to a bi-axial elongation which deforms the spherical part of the droplet converting it into an elongated shape. This elongated shape blends into a tail and the droplet is converted into a viscous elongated teardrop. The tail is then subjected to a uniaxial extensional flow under the action of elongational stresses along the length of the tail. This extensional flow is counteracted by the shear stresses acting on the interface between the tail and the outer surrounding fluid. This interaction will determine the tail breakup. The influence of the elastic properties of the surrounding fluid and the extensional viscosity of the droplet will be responsible for the length and thickness of the tail as well as for its breakup mechanism.

✉ Baltasar Mena
mena@unam.mx

Bernardo Figueroa-Espinoza
bfigueroae@iingen.unam.mx

1 Laboratorio de Ingeniería y Procesos Costeros, Instituto de Ingeniería, UNAM, Puerto de Abrigo S/N, Sisal, Yucatán 97355, Mexico

2 School of Engineering, Brown University, Providence, RI, USA

Keywords Non-Newtonian droplets · Viscoelastic fluids · Critical volume · Tail breakup · Extensional flow · Velocity jump · Negative wake

Introduction

The flow around Newtonian droplets rising in viscoelastic fluids is a popular, well-studied, and fairly well-understood problem. The simplest case is being the flow around rising air bubbles in a non-Newtonian fluid (see for example Caswell et al. 2004, Herrera-Velarde et al. 2003, Soto et al. 2006). Some characteristic phenomena pertaining to such a case include the appearance of a jump discontinuity in velocity at a particular volume (known as the critical volume). A negative wake also appears in many situations which is also related to the jump discontinuity and to the change in bubble shape as it travels upwards in the viscoelastic medium that surrounds it. The viscoelastic properties of the surrounding fluid are responsible for the change in bubble shape, in particular the normal stresses acting on the surface of the bubble as well as the shear-dependent viscosity of the outer fluid (Caswell et al. 2004, Herrera-Velarde et al. 2003, Soto et al. 2006, Arigo and McKinley 1998, Rodrigue and De Kee 1998, Rodrigue et al. 1998).

However, the flow of non-Newtonian deformable droplets moving in a Newtonian fluid or in a viscoelastic medium is not well documented. In this case, many interesting situations arise. These are the topic of this experimental research.

First of all, if the droplet is viscoelastic but the fluid around it is Newtonian, no interesting phenomena occur; the droplet will attain its spherical or slightly elongated form and travel as a solid object.

On the other hand, if the droplet is viscoelastic and it travels in a viscoelastic medium, several different cases are possible. These will be examined experimentally and discussed below.

Experimental arrangement

The experimental setup consists of an acrylic vertical container 80 cm in height with a square cross section of 15 cm × 15 cm. This container houses the external fluid through which the droplet will travel. The droplets are injected through the bottom of the container using a syringe pump through orifices of variable diameter. The volume of the injected droplet is controlled by the rate at which the fluid is pumped through the syringe as it fills a small receptacle adjacent to the container; droplet volumes varied from 1 to 15 ml. A CCD (GigE, IDS) connected to a computer captures the droplet images. The camera is mounted on a traveling system with a controlled speed, which coincides with the terminal velocity of the droplet. Typical velocities varied from 0.1 to 15 mm/s.

In order to study the flow around the droplets, a PIV system (Dantec™ Dynamics) was used. Hollow glass silver-coated particles were used as tracers. Diameters vary from 10 to 150 μm with a neutral buoyancy in the container. Several other cameras were employed throughout the experiments as well as some laser arrangements prior to the arrival of the Dantec™ PIV system.

The system is depicted schematically in Fig. 1.

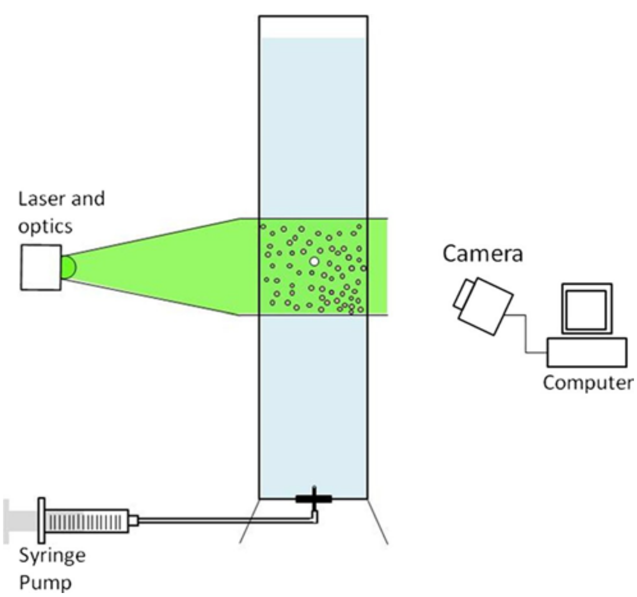

Fig. 1 Experimental setup

Experimental fluids

Newtonian fluids

Air, water, and silicone oil of various viscosities (Dow Corning)

Non-Newtonian fluids

1. Solution A: Poly-isobutylene (0.5 %) dissolved in a mixture of polybutene oil (51.3 %) and decalin (48.7 %). This particular fluid (known as S1) was widely used as a universal test fluid a few decades ago and its properties are well known; in particular, an extensive set of measurements were reported for the elongational properties of this solution (Hudson and Ferguson 1994, Willenbacher and Hingmann 1994). This fluid does not exhibit a yield stress. The components are listed as follows:

   & PIB characteristics: Sigma-Aldrich; Mw approx. 1,000,000, Mn approx. 600,000, Mv approx. 1,200,000, density 0.896 g/ml
   & Polybutene oil: Sigma-Aldrich; Mw 920, viscosity 200–250 cst@100oC, density 0.89 g/ml
   & Decalin: Sigma-Aldrich; Mn approx. 138.25, density 0.896 g/ml

2. Solution C: Polyacrylamide (0.3 % Separan AP-30) in distilled water. This particular fluid has been used by our group in many previous experiments for flow around spheres and bubbles (Caswell et al. 2004, Herrera-Velarde et al. 2003, Manero and Mena 1981, Mena et al. 1987, Broadbent and Mena 1974). Polyacrylamide: Dow-Chemical; Separan AP-30; Mw 71.08 g/mol.mo mol. weight 1–4 × 10^6.

   Note: Polyacrylamide solutions have been reported to exhibit yield stress (Ghannam and Esmail 1998). This was not detected in our experimental results but was rightfully noted by one of the referees.
3. Solution D: Polyox (0.5 %) in distilled water. This solution has a similar viscosity behavior as solution C with different elastic characteristics (Sigma-Aldrich, average mol. weight between 4 × 10^5 and 4 × 10^6)

Solutions C and D will help to establish the influence of the elasticity of the outer fluid upon the deformation of the droplet. The viscoelastic droplet in these experiments was always made with S1 fluid.

The preparation and mixing techniques for the fluids may be found in Ortiz (2015), Hudson and Ferguson (1994), and Willenbacher and Hingmann (1994).

Rheological characteristics

The rheological properties of the experimental fluids were measured using a stress-controlled T.A. Instruments ARG-2 rheometer. The geometries used in the oscillatory measurements were cone and plate and parallel plates. Surface tension measurements were performed using a Wilhelmy balance with a Du Nouy ring and with pendant drop method. The purpose was to examine the influence of the outer fluids (C and D) in the deformation and breakup of the deformable S1 droplet. The rheological curves are summarized in Figs. 2, 3, 4, and 5.

Experimental results

Case 1. Newtonian droplets in non-Newtonian fluids

Air bubbles and water droplets

Most results in the literature are for air bubbles rising in non-Newtonian fluids. There is a wealth of information with regard to the topic. For a compilation, see for example Caswell et al. 2004.

However, in order to verify the validity of the experimental system, air and water droplets were injected as Newtonian fluids in a viscoelastic aqueous Polyox 5 % solution. As expected, both air bubbles and water droplets presented the usual balloon-like shapes as reported in the literature (Caswell et al. 2004, Herrera-Velarde et al. 2003, Soto et al. 2006, Rodrigue and De Kee 1998, Rodrigue et al. 1998, Astarita and Apuzzo 1965, Hassager 1979, Bisgaard and Hassager 1982).

Viscous Newtonian droplets

The next validating experiment is with oil droplets. As can be seen in Fig. 6, the droplet velocity varies linearly with its volume until a critical value is reached; at that point, a jump in velocity occurs (in the present case around a volume of 2.9 ml). It should be noticed that since the driving force for the droplet is due to the density difference between the droplet and the external fluid, the terminal velocity is very small. The viscous forces are much larger than those of water or air; nevertheless, a small jump in velocity appears at a critical volume. This is shown in Fig. 6. The range for Reynolds number is between 0.01 and 0.1 whilst the range of Weissenberg number was from 0.1 to 15.

Additionally, a tail appears at the bottom of the droplet. If the volume of the droplet is increased further beyond the critical volume at which the tail appears, the droplet will eventually eject a small amount of the fluid by breaking its tail. This is shown in Fig. 7.

It can be inferred that if a droplet is allowed to travel a large-enough distance, it will slowly eject the volume in excess of the critical value (in the form of satellite droplets), until the volume is reduced once again to its critical value and the droplet will not have a tail anymore. Therefore for the breakup of the tail to occur, the critical volume has to be exceeded. Additionally, as soon as the critical volume is reached, a negative wake will appear.

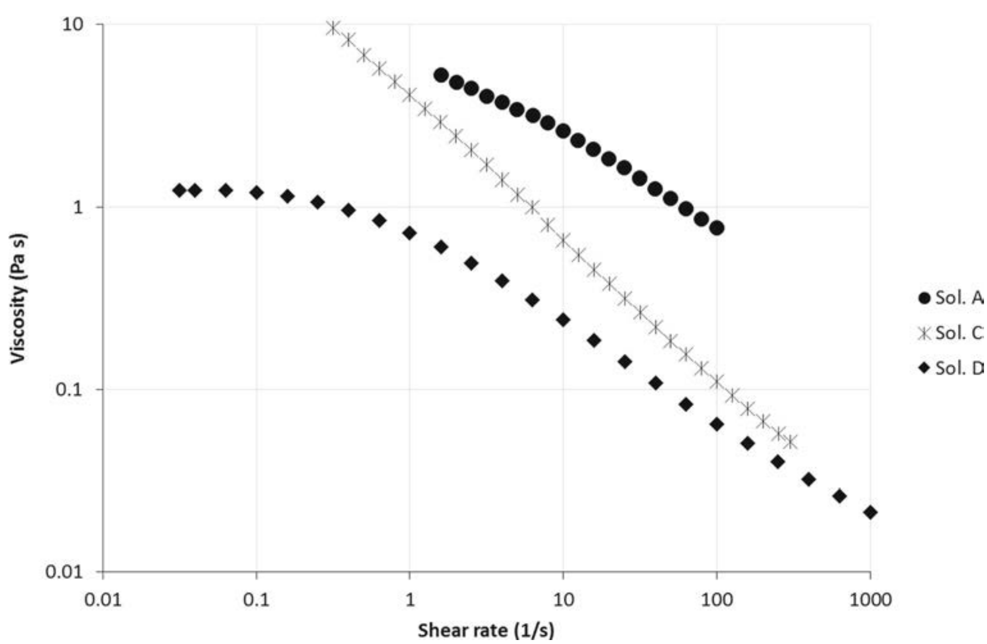

Fig. 2 Viscosity (Pa s) as a function of shear rate (1/s)

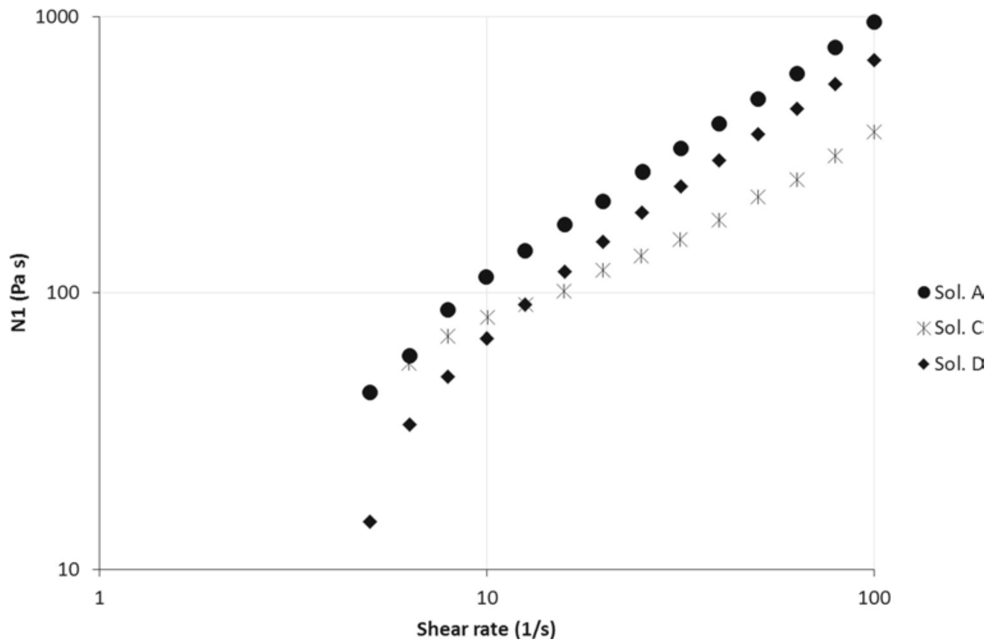

Fig. 3 First normal stress difference N1 (Pa s) as a function of shear rate (1/s)

Figure 8 shows a PIV image of the appearance of the negative wake at the critical volume for a silicone oil droplet rising through solution D.

Case 2. Non-Newtonian droplets in viscoelastic fluids

The flow of non-Newtonian (viscoelastic) droplets traveling through non-Newtonian fluids is not a very well-documented problem. In this section, we will discuss the results of viscoelastic droplets (PIB 0.5 % in polybutene oil) traveling in two different viscoelastic outer fluids.

PIB 0.5 % in polybutene oil (solution A) as a droplet with a Separan 0.3 % aqueous solution (solution C) as an outer fluid

Solution A (PIB 0.5 % in polybutene oil) droplets are injected at the bottom of a container filled with solution C in order to investigate a viscoelastic droplet traveling in a viscoelastic fluid. Similar to the cases seen with Newtonian droplets, formations of tails are observed at a certain volume, called the critical volume (Fig. 9). However, in this case, the cusp at the end of the droplet is smooth and the tail does not break up

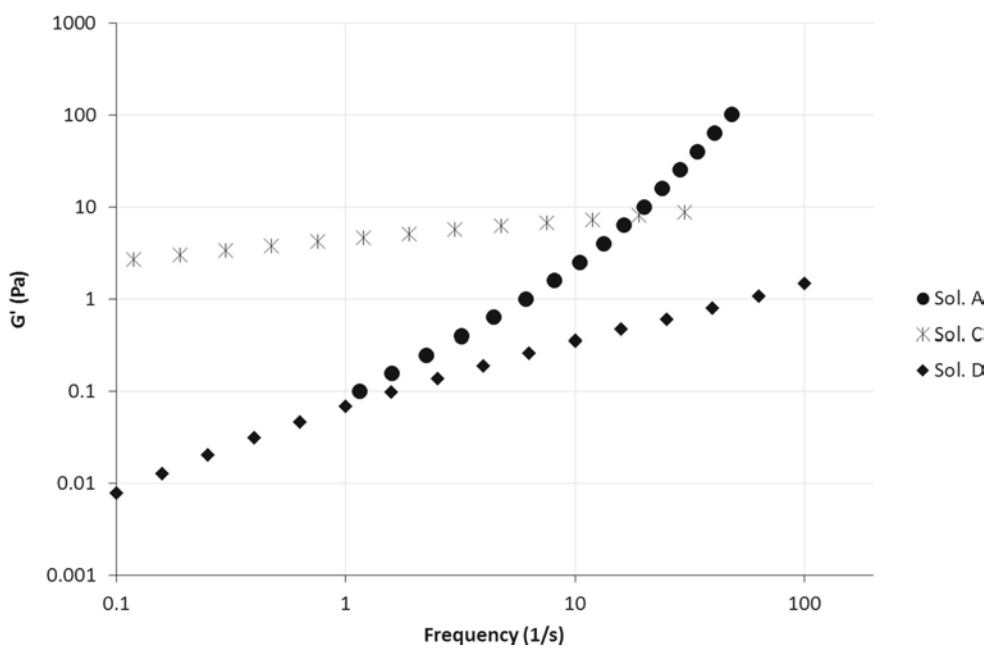

Fig. 4 G′ (Pa) as a function of frequency (1/s)

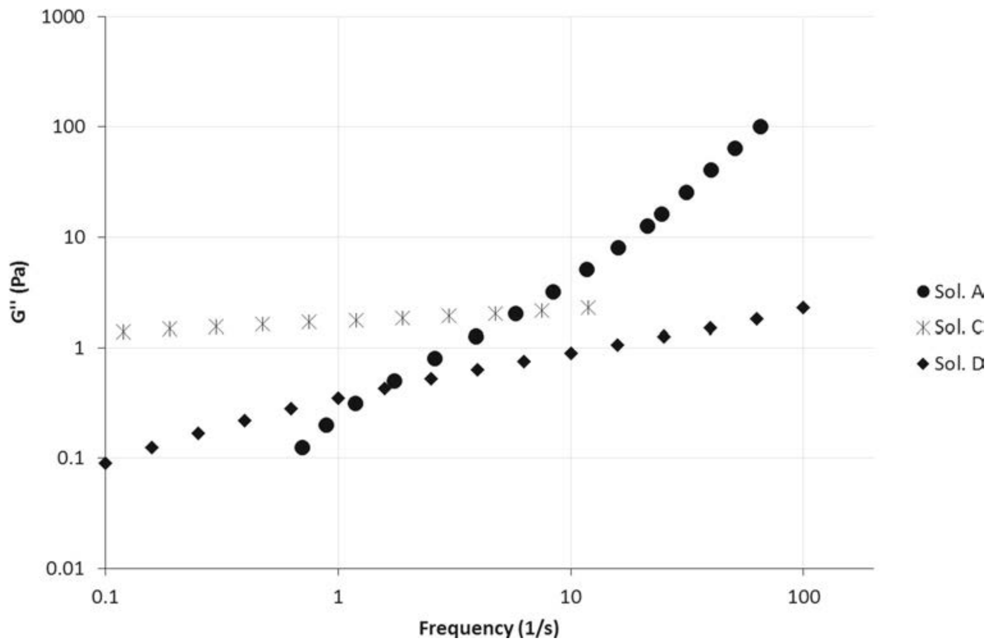

Fig. 5 G″ (Pa) as a function of frequency (1/s)

easily; instead, it extends as the droplet travels towards the top of the container. The droplet adopts a tear-like elongated shape that may extend a long distance.

The following figures show the sequence of elongation and deformation of the tail as the droplet travels.

In order to better understand the deformation process, it is convenient to divide the droplet into different sections. The first section is the region of the head (I). A second section is the tail section (II). This is depicted in Fig. 10 for a larger volume droplet (8 ml).

In region I, we may observe that just after the head, a wake is formed as in the case of a Newtonian droplet, and due to the elastic properties of the surrounding fluid, a recirculating zone appears in the opposite direction to the flow; this is known as the "negative wake". Figure 10 (I) shows the appearance of the negative wake and the formation of the tail (similar results were found for volumes for up to 14 ml).

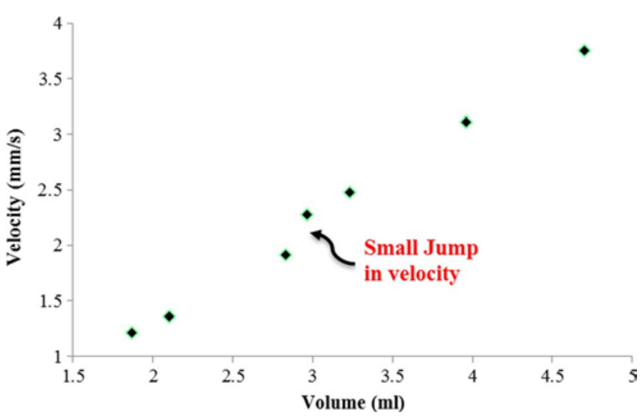

Fig. 6 Silicone oil droplets (Newtonian) rising in a Polyox 0.5 % aqueous solution D (viscoelastic) fluid

This negative wake tends to stretch the tail in opposite direction to the motion of the droplet, creating a region of uniaxial extension. In this section, the elongational stress competes with the shear stress along the tail. It is the balance between these forces that dominates the phenomenon and will eventually determine whether the tail will break or not.

In Fig. 10, region II, it may be observed that the negative wake decreases in magnitude until it finally disappears and is influenced by the lump at the end of the tail just before breakup begins.

Figure 11 shows the breakup mechanism of the tail. The length of the tail will depend on the elongational characteristics of the fluid in the droplet and on the viscoelastic characteristics of the surrounding outer fluid. If the outer fluid is very viscous and highly elastic, the tail region may extend a long distance without breaking. The distance will depend, of course, on the tensile properties of the droplet. The surface tension between the S1 fluid and the surrounding fluids C and D was very similar (around 58 mN/m). The capillary number varied for each case but very little (between 0.15 and 0.2). In every case, the Weber number was close to 0.01. It should be noticed that since the difference in density between the droplet and the outer fluid is very small, the rising velocity of the droplet is also very small (less than 1 mm/s); consequently, the characteristic shear rate is also very small (around 0.1 s^{-1}) for the droplet volumes considered. In summary, all things considered, the effects of surface tension upon the flow were kept as constant as possible. Inertia effects were also kept very small. The dominating forces are mainly elastic and viscous.

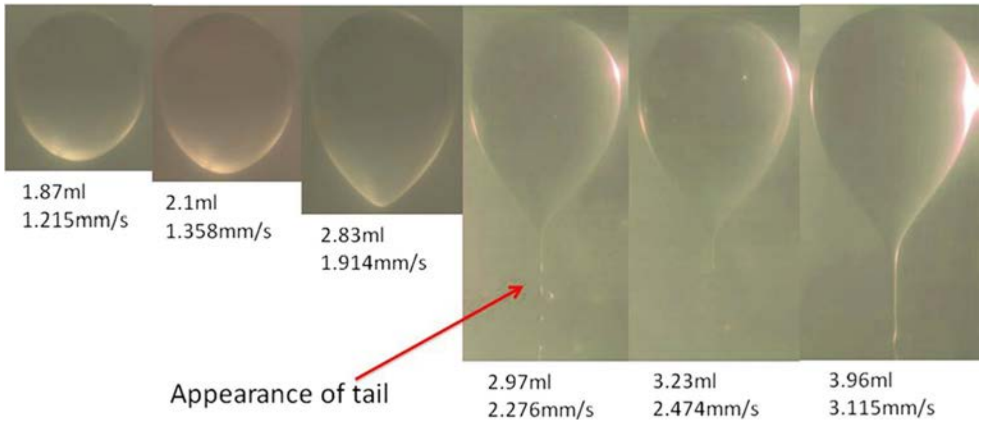

Fig. 7 Captured images of (Newtonian) silicone oil droplets traveling in a Polyox 0.5 % aqueous solution (solution D) at different volumes

Figure 12 shows the typical behavior of a droplet (solution A) in the Polyox (solution D). The distinct regions are depicted in the photograph.

In the uniaxial extension region, the tail forms a filament of slowly decaying radius, as shown in Fig. 12. In fact, one may consider the cross-sectional velocity profile as uniform. By measuring the change in filament diameter, the rate of extension of the filament may be calculated (Cruz-Mena et al. 2002, Rios et al. 2002) as follows:

$$\varepsilon = \frac{\partial u}{\partial z} \quad (1)$$

where u is the upward droplet velocity. If the velocity profile is considered uniform in the cross section of the filament, the rate of extension may be approximated by measuring the velocity difference between two sections of the filament divided by the length between the sections (Rios et al. 2002, Manero and Mena 1981).

If the first normal stress difference in simple shear is given by

$$N_1 = \left(\tau_{xx} - \tau_{yy}\right) \quad (2)$$

and the normal stress difference in uniaxial extension is

$$\Delta\tau_{ext} = (\tau_{zz} - \tau_{rr}) = \eta_{ext}(\varepsilon)\varepsilon; \quad (3)$$

then the ratio between Eqs. 2 and 3 will determine the condition for the formation of a negative wake (see Arigo and McKinley 1998), where the transient extensional viscosity η_{ext} will depend on the extension rate, and the shear viscosity η will be a function of a typical rate of shear.

$$\gamma = \frac{u}{d} \quad (4)$$

where d is the filament cross section diameter. The ratio between the normal stress difference in shear and the normal

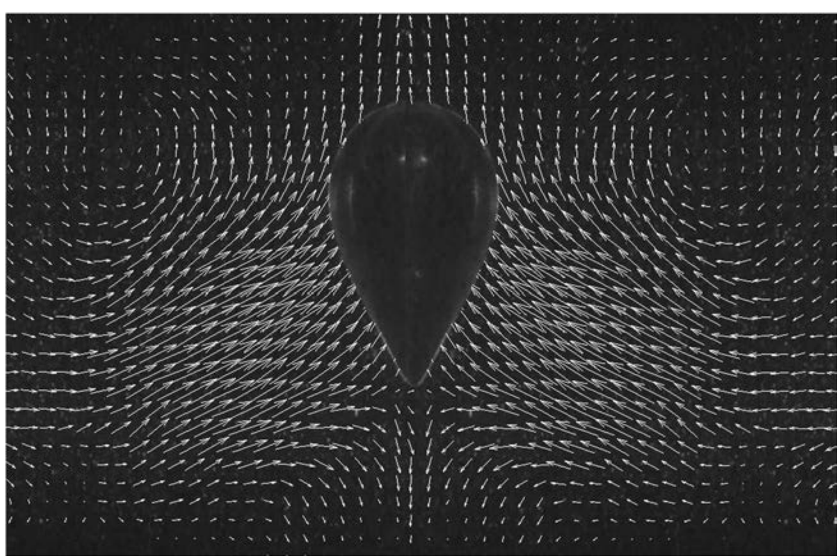

Fig. 8 Appearance of negative wake at the critical volume

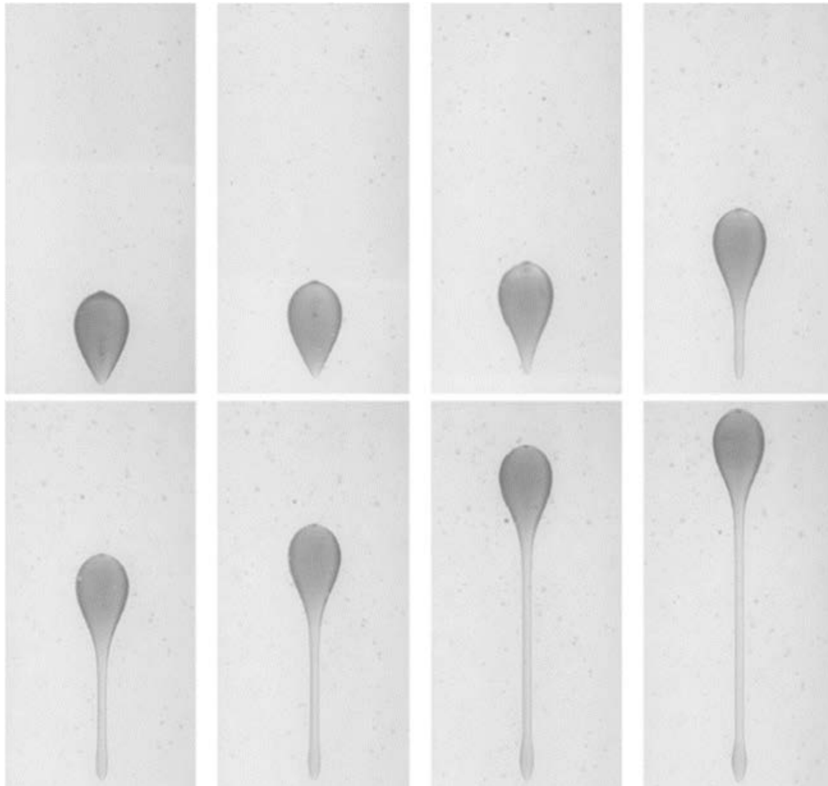

Fig. 9 Evolution of the deformation of a small 3 ml PIB (solution A) droplet traveling upwards in a Separan 0.3 % aqueous solution (solution C)

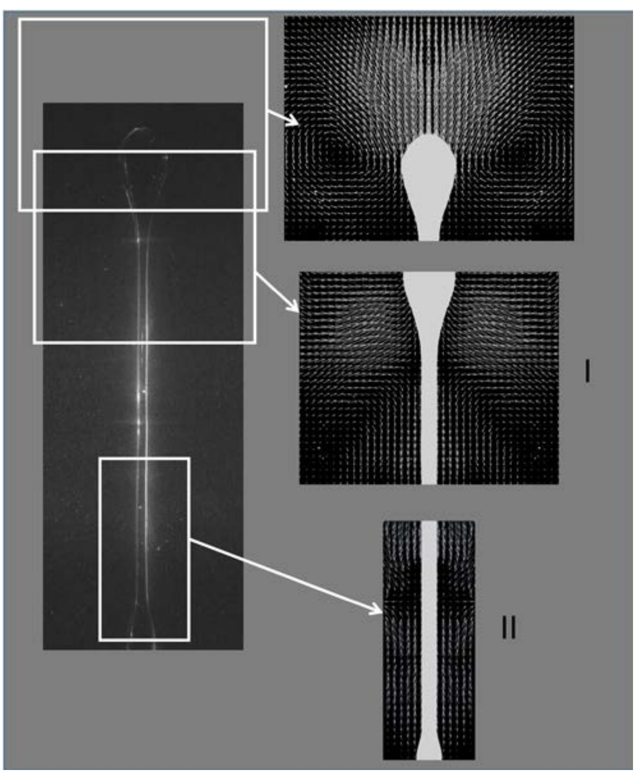

Fig. 10 The deformation of a viscoelastic sol. A (8 ml droplet) is divided into two regions: I (head) and II (tail). PIV measurements are shown for each section

stress difference in uniaxial extension will determine the condition for the formation of the negative wake (Arigo and McKinley 1998).

$$\frac{N_1}{\Delta\tau_{ext}} \propto \frac{W_e}{T_r} \quad (5)$$

Here, $W_e = \frac{\lambda}{d} u$ is the Weissenberg number based on the relaxation time of the fluid at the typical rate of shear γ and T_r is the Trouton ratio evaluated at the corresponding extension rate.

The force balance in the filament region will be given by Arigo and McKinley 1998:

$$f_z = \frac{\partial \tau_{zz}}{\partial z} + \frac{1}{r}\frac{\partial}{\partial r}(r\tau_{rz}) \quad (6)$$

where τ_{zz} decays as $z \to -\infty$; $\frac{\partial \tau_{zz}}{\partial z} > 0$

τ_{rz} varies from 0 at the center line and becomes more negative as the radial coordinate increases. Therefore, a negative f_z corresponds to a driving force for a negative wake (Arigo and McKinley 1998).

The force could then be calculated from a measured value of η_{ext} corresponding to a given characteristic shear rate. Such measurements are possible using a system such as the one described in Cruz-Mena et al. 2002 and Rios et al. 2002.

The extensional stress decays as the filament length increases and the shear stress becomes larger. These competing stresses will determine the type of breakup of the tail.

If however the tail is long and thick, the change in filament diameter is almost zero and the tail does not break. In the experimental arrangement, due to the finite dimensions, the tail does not break; nevertheless, for a large-enough container, the tail would eventually break into satellite droplets.

In summary, for a given volume above the critical one, the influence of the elastic properties of the surrounding fluid and the extensional viscosity of the droplet will be responsible for the length of the tail as well as for the breakup system.

Conclusions

Newtonian droplets

In the case of Newtonian droplets such as air bubbles, water droplets, and oil droplets traveling in viscoelastic media, a critical volume exists at which there is a change in shape of the droplet from an oval or convex spheroid shape to a geometry with a sharp cusped end. This change in shape is due to the presence of the elastic normal stresses of the outer viscoelastic fluid, enhanced by the shear-dependent viscosity. As a result, this change of curvature at the end of the droplet gives rise to the appearance of a tail as well as a jump in the velocity. Simultaneously, a flow reversal appears behind the droplet commonly known as the negative wake. The length of the tail, the magnitude of the velocity jump, and the duration of the negative wake will depend entirely on the viscoelastic properties of the surrounding fluid. The tail may extend some distance but will eventually break into small droplets.

Viscoelastic droplets

In the case of a viscoelastic droplet traveling through a viscoelastic fluid, several major differences appear. Although a critical volume exists, experimental data showed no measurable jump in velocity. Nevertheless, a tail appears as well as a negative wake. For large-enough volumes, the thickness of the tail is much larger than that for the Newtonian droplets; this is also true for the magnitude of the negative wake and for the extension of the tail. The head of the droplet is subjected to a bi-axial elongation which deforms the spherical part of the droplet converting it into an elongated shape. This elongated shape blends into a tail and the droplet is converted into a semi-solid elongated teardrop. The tail is then subjected to a uniaxial extensional flow under the action of elongational stresses along the length of the tail. This elongational flow is counteracted by the shear stresses acting on the interface and to a lesser extent by the negative wake. This interaction will determine the breakup mechanism.

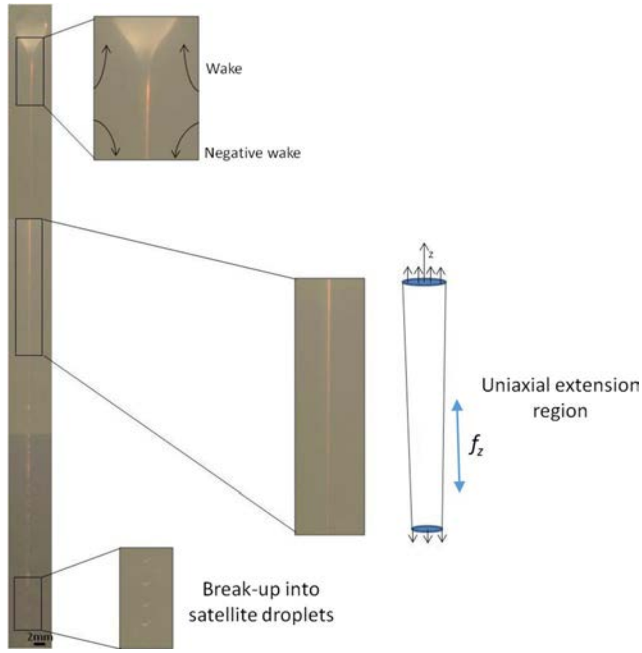

Fig. 12 Schematic description of the observed uniaxial tension on the droplet in the distinct regions of interest

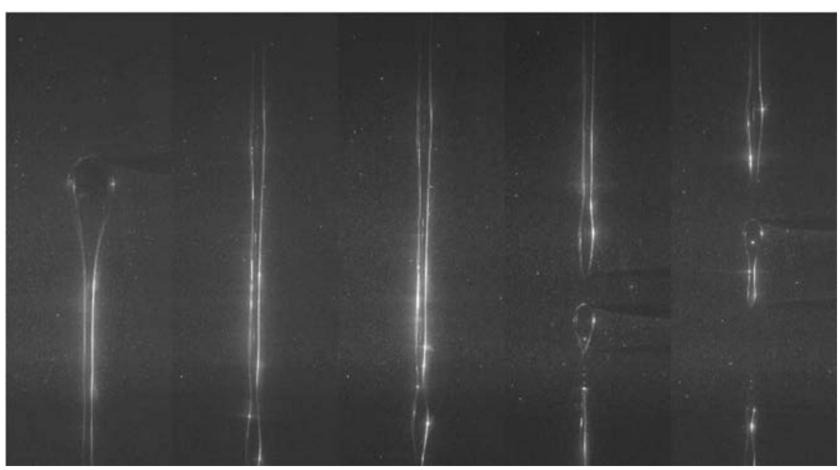

Fig. 11 Deformation sequence for a 12-ml droplet. The tail finally breaks into small satellite droplets

The tail may vary in diameter as it is elongated as the droplet rises. This section may be useful as a possible measure of elongational unidirectional flow or to determine the extensional viscosity of the fluid in the droplet (see for example Cruz-Mena et al. 2002, Rios et al. 2002).

In the experiments reported here, the container was not long enough to allow us to examine whether the tail would eventually break or if the droplet would continue its motion as a solid body. This and other related matters will be the subject of future investigation.

Acknowledgments The authors wish to acknowledge Prof. K. Breuer for allowing us to use his lab facilities during the sabbatical leave of B.M. at Brown University. Also, we acknowledge the grant given by DGAPA (UNAM) through project PAPIIT IN106512. Useful comments from the referees are also gratefully acknowledged.

References

Arigo MT, McKinley GH (1998) An experimental investigation of negative wakes behind spheres settling in a shear-thinning viscoelastic fluid. Rheol Acta 37:307–327

Astarita G, Apuzzo G (1965) Motion of gas bubbles in non-Newtonian liquids. AICHE J 11:815–820

Bisgaard C, Hassager O (1982) An experimental investigation of velocity fields around spheres and bubbles moving in non-Newtonian liquids. Rheol Acta 21:537

Broadbent J, Mena B (1974) Slow flow of an elastico-viscous fluid past cylinders and spheres. Chem Eng J 8(1):11–19

Caswell B, Manero O and Mena B (2004) Recent developments on the slow viscoelastic flow past spheres and bubbles. In: DM Binding and K Walters (eds.) Rheology reviews. 197–223.

Cruz-Mena J, Serrania F, Mena B (2002) Some theoretical and experimental relations between simple shearing and simple extension. Rev Mex Fis 48(S1):51–56

Ghannam MT, Esmail MN (1998) Rheological properties of aqueous polyacrylamide solutions. J Appl Polym Sci 69:1587–1597

Hassager O (1979) Negative wake behind bubbles in non-Newtonian liquids. Nature 279:402

Herrera-Velarde JR, Zenit R, Chehata D, Mena B (2003) The flow of non-Newtonian fluids around bubbles and its connection to the jump discontinuity. J Non-Newtonian Fluid Mech 111:199–209

Hudson NE, Ferguson J (1994) The anomalous shear flow properties of S1. J Non-Newtonian Fluid Mech 52:105–119

Manero O, Mena B (1981) On the slow flow of viscoelastic fluids past a circular cylinder. J Non-Newtonian Fluid Mech 9(3–4):379–387

Mena B, Manero O, Leal LG (1987) The influence of rheological properties on the slow flow past spheres. J Non-Newtonian Fluid Mech 26(2):247–275

Ortiz SL (2015) Thesis, Fac. Ingenieria, UNAM

Rios S, Diaz J, Galindo A, Soto E, Calderas F, Mena B (2002) Instrumentation and start up of a new elongational rheometer with a preshearing history. Rev Scientific Instruments 73(8):3007–3011

Rodrigue D, De Kee D (1998) Bubble velocity jump discontinuity in polyacrylamide solutions; a photographic study. Rheol Acta 37:307–327

Rodrigue D, De Kee D, Chan Man Fong C (1998) Bubble velocities: further developments on the jump discontinuity. J Non-Newtonian Fluid Mech 79:45–55

Soto E, Goujon C, Zenit R, Manero O (2006) A study of velocity discontinuity for single air bubbles rising in an associative polymer. Phys Fluids 18:121510

Willenbacher N, Hingmann R (1994) Shear and elongational flow properties of fluid S1. J Non-Newtonian Fluid Mech 52:163–176